Hindawi
Advances in Civil Engineering
Volume 2020, Article ID 8824445, 12 pages
https://doi.org/10.1155/2020/8824445

Research Article

Amplification of Seismic Response in Poroviscoelastic Soil Layer

Liming Yang,[1,2] Junhui Luo ,[1,2] Weiyun Chen,[3] and Yumin Mou[3]

[1]*Guangxi Xinfazhan Communications Group Co., Ltd., Nanning, Guangxi 530029, China*
[2]*Guangxi Communication Design Group Co., Ltd., Nanning, Guangxi 530029, China*
[3]*Institute of Geotechnical Engineering, Nanjing Tech University, Nanjing 210009, China*

Correspondence should be addressed to Junhui Luo; jhluo85@hotmail.com

Received 24 April 2020; Revised 2 June 2020; Accepted 16 June 2020; Published 11 July 2020

Academic Editor: Peixin Shi

The time-dependent behaviour of saturated soils under static and dynamic loading is generally attributed to the flow-dependent and viscous behaviour of pore fluid. However, the intrinsic energy dissipative effects from the flow-independent viscoelastic behaviour of solid skeleton are not always considered. In this study, the effect of flow-independent viscoelastic behaviour on the seismic amplification of ground soil in vertical and horizontal directions is studied based on a two-phase poroviscoelastic model. A generalized Kelvin–Voigt model is used to define the effective stress in the soils, and the compressibilities of both solid skeleton and pore fluid are considered. The seismic-induced dynamic displacements are analytically derived and are shown to depend on soil layer thickness, soil properties, and ground motion parameters. The formulation neglecting the viscoelastic behaviour of solid skeleton could overestimate both the vertical and horizontal motion amplifications at the surface of ground soil. In addition, the seismic responses of viscoelastic soils are demonstrated to be closely related to the saturation state of surface soil.

1. Introduction

The characteristics of seismic ground motions at a specified site are significantly affected by site conditions such as soil properties and topography [1, 2]. In practical engineering, the evaluation of site response to earthquakes is usually employed as the input motions for seismic design of engineering structures. In addition, the amplification of seismic response is significant in the assessment of seismic hazard such as rock-fall and slope collapse, as it could have a marked impact on the damage patterns over large areas even due to a moderate earthquake [3–5]. An extensive study has been conducted on the site response using the shaking table test [6], numerical method [7, 8], and the analytical method [9–14].

In general, the seismic waves propagating in the isotropic Earth are associated with the vibrating direction of the substrate bedrock. So far, a great number of models which are based on existing seismic records have been proposed for horizontal site response. However, the study on the amplification effect of vertical motion is quiet limited. This is perhaps due to the fact that the engineering structures are sufficiently resistant to the vertical earthquake action, which has smaller magnitude but becomes more obvious in high frequency range [15]. The phenomenon of structural damage under the action strong vertical earthquake has been continuously observed [16, 17], and ignoring the effect of vertical motion may lead to underestimation of ground motion site response [18]. In the quasi-static study, the peak vertical acceleration is assumed to be 1/2 or 2/3 of the peak horizontal acceleration [19, 20], which is not always reasonable, because the ratio between the peak values of vertical and horizontal accelerations was found to be greater than 1.5 in Northridge earthquake [21]. Therefore, the influence of vertical seismic motion on the dynamic analysis of important structures should be taken into account.

It is widely accepted that the two-phase porous theory presented by Biot [22] is an effective approach to analyze the dynamic response of fluid-saturated soils [11, 23–26]. In the classical porous medium theory, only the resistance of fluid viscosity is considered, while the behaviour of the solid skeleton is assumed to be elastic [11, 23–26]. In general, the Earth media friction attenuates the energy of seismic wave and thus regarding Earth medium as viscoelasticity is more

appropriate than as elasticity. It has been found that the damping for the fluid-saturated soils is greater than that in the dry state [27, 28]. In addition to the fluid-solid coupling in the soils, the damping of solid skeleton also causes energy dissipation. However, insufficient attention has been paid on the viscoelastic character of poroelastic materials in practical engineering. Following the Biot theory, Bardet [29] developed a viscoelastic model for the dynamic behaviour of saturated soils, which was derived from the velocity and attenuation of compressional and shear waves. In Xie et al. [30], the dynamic behaviour of partially sealed tunnel in viscoelastic soils is studied with the aid of Kelvin–Voigt model.

In the present paper, the effective stress of soil skeleton is characterized by using a Kelvin–Voigt model, which can be represented by a spring and damper arranged in parallel. The arising two-phase viscoelastic model could describe both the flow-independent and flow-dependent dissipative phenomena. The various response variables in the cases of vertical and horizontal seismic motion are obtained analytically. A set of parametric analysis is then carried out to analyze the influence of critical parameters on the seismic wave propagation and the motion amplification in the viscoelastic soil layer.

2. Governing Equations for Viscoelastic Soil

In general, soil is a so-called damping material as a part of energy of the wave which will dissipate during the propagation [31]. The viscoelasticity of soil skeleton is described by Kelvin–Voigt model and the stress-strain relationship is [32]

$$\sigma'_{ij} = \lambda_e e\delta_{ij} + 2\mu_e\varepsilon_{ij} + \lambda_v\frac{\partial e}{\partial t}\delta_{ij} + 2\mu_v\frac{\partial \varepsilon_{ij}}{\partial t}, \tag{1}$$

where σ'_{ij} is the effective stress, δ_{ij} is Kronecker delta, μ_e and λ_e are Lamé elastic moduli, λ_v and μ_v are the dilatant constant and shear constant of the viscoelastic soil, e denotes the volumetric strain of solid skeleton, and the strain ε_{ij} is expressed as

$$\varepsilon_{ij} = \frac{1}{2}\left(u_{i,j} + u_{j,i}\right), \tag{2}$$

where $u_{i,j}$ and $u_{j,i}$ are the derivatives of the soil skeleton displacement with respect to spatial coordinates.

Based on the continuity of flow condition, the constitutive equation for compressible fluid in the pores is

$$p = M\zeta - \alpha Me, \tag{3}$$

where p is the pressure of the interstitial fluid, $\zeta = -\overline{w}_{i,j}$ indicates volumetric strains of fluid, $\overline{w}$ is the average displacement of pore fluid relative to the solid and can be expressed as $\overline{w} = n(w - u)$, n is the soil porosity, and u and w are the displacements of solid skeleton and pore fluid, respectively. M and α are the coefficients related to the compressibility of the grains and fluid:

$$\alpha = 1 - \frac{K_b}{K_s},$$

$$M = \frac{K_s^2}{K_{\ d} - K_b}, \tag{4}$$

$$K_d = K_s\left[1 + n\left(\frac{K_s}{K_f} - 1\right)\right],$$

where K_s, K_b, and K_f are the bulk moduli of solid grains, solid skeleton, and pore fluid, respectively.

In the case of high saturation (e.g., Sr > 95%), one may treat the air-water mixture as a homogeneous pore fluid by assuming that the air exists in the form of bubbles. K_f is the bulk modulus of the homogeneous fluid expressed as [33]

$$K_f = \frac{1}{(1/K_w) + ((1 - S_r)/p_{w0})}, \tag{5}$$

where S_r is the saturation degree, p_{w0} is the absolute fluid pressure, and K_w is the true bulk modulus of water.

Neglecting the body forces, the overall equilibrium equation for a unit total volume could be expressed as

$$\sigma'_{ij,j} - \alpha\delta_{ij}p_{,j} = \rho\frac{\partial^2 u_i}{\partial t^2} + \rho_f\frac{\partial^2 \overline{w}_i}{\partial t^2}, \tag{6}$$

where ρ is the total density expressed as $\rho = (1 - n)\rho_s + n\rho_f$, ρ_s is the density of the soil grain, and ρ_f denotes the fluid density. It should be noted that tension is positive for the pore pressure.

2.1. Equilibrium Equation for the Liquid Phase. The equilibrium equation for the liquid phase is

$$-p_{,j} = \rho_f\ddot{u}_i + \left(\frac{\rho_f}{n}\right)\ddot{\overline{w}}_i + b\dot{\overline{w}}_i, \tag{7}$$

where b is the coefficient representing the resisting forces from the fluid-solid coupling and could be expressed as (η/K), where η denotes the fluid viscosity and K is the permeability in the unit m^2. It is noted that the third term at the right side of equation (7) could reveal the viscous coupling which involves viscous resisting forces between the pore fluid and solid skeleton. Compared with the flow-independent dissipative effects from the viscosity of solid skeleton itself, this flow-dependent viscosity is also significant because it generally results in the dispersion and dissipation of seismic waves [34]. When the wavelength is far greater than pore size, the coefficient b could be defined as the ratio of unit weight of pore fluid (γ_f) to coefficient of permeability (hydraulic conductivity, K_D); that is, $b = (\gamma_f/K_D)$.

Then, the governing equations for the poroviscoelastic medium could be derived as

$$\mu_e \nabla^2 u + \mu_v \nabla^2 \dot{u} + \left(\lambda_e + \mu_e + \alpha^2 M\right) \nabla (\nabla \times u) + (\lambda_v + \mu_v) \cdot \nabla (\nabla \times \dot{u}) + \alpha M \nabla (\nabla \times w) = \rho \ddot{u} + \rho_f \ddot{\overline{w}}, \tag{8}$$

$$\alpha M \nabla (\nabla \times u) + M \nabla (\nabla \times w) = \rho_f \ddot{u} + \left(\frac{\rho_f}{n}\right) \ddot{\overline{w}} + b \dot{\overline{w}}. \tag{9}$$

3. Problem Definition

In this section, the steady-state displacement excitations are assumed to act at the bottom of the soil layer in vertical and horizontal directions, respectively. As shown in Figure 1, the soil is treated as poroviscoelastic medium with thickness L. The soil surface is stress-free and free-draining, while its base is considered as impermeable and rigid.

3.1. Vertical Motion. When the vibration of bedrock is vertical, the dynamic motion of particles in the soils could be simplified as a one-dimensional problem. Then, equations (8) and (9) can be conveniently reduced to

$$\left(\lambda_e + 2\mu_e + \alpha^2 M\right) \frac{\partial^2 u}{\partial z^2} + (\lambda_v + 2\mu_v) \frac{\partial^3 u}{\partial z^2 \partial t} + \alpha M \frac{\partial^2 \overline{w}}{\partial z^2} - \rho \frac{\partial^2 u}{\partial t^2} - \rho_f \frac{\partial^2 \overline{w}}{\partial t^2} = 0, \tag{10}$$

$$-\alpha M \frac{\partial^2 u}{\partial z^2} - M \frac{\partial^2 \overline{w}}{\partial z^2} + \rho_f \frac{\partial^2 u}{\partial t^2} + \frac{\rho_f}{n} \frac{\partial^2 \overline{w}}{\partial t^2} + b \frac{\partial \overline{w}}{\partial t} = 0. \tag{11}$$

Then the displacement of soil skeleton could be further obtained as

$$\frac{\partial^4 u}{\partial t^4} + a_1 \frac{\partial^5 u}{\partial z^2 \partial t^3} + a_2 \frac{\partial^3 u}{\partial t^3} + a_3 \frac{\partial^4 u}{\partial z^2 \partial t^2} + a_4 \frac{\partial^3 u}{\partial z^2 \partial t} + a_5 \frac{\partial^5 u}{\partial z^4 \partial t} + a_6 \frac{\partial^4 u}{\partial z^4} = 0, \tag{12}$$

in which

$$a_1 = \frac{\lambda_v + 2\mu_v}{n\rho_f - \rho},$$

$$a_2 = -\frac{\rho n b}{\rho_f \left(n\rho_f - \rho\right)},$$

$$a_3 = \frac{nb\left(\lambda_v + 2\mu_v\right)}{\rho_f \left(n\rho_f - \rho\right)} + \frac{\lambda_e + 2\mu_e + M\left(\alpha^2 + \left(n\rho/\rho_f\right) - 2\alpha n\right)}{n\rho_f - \rho},$$

$$a_4 = \frac{nb\left(\lambda_e + 2\mu_e + \alpha^2 M\right)}{\rho_f \left(n\rho_f - \rho\right)},$$

$$a_5 = -\frac{Mn\left(\lambda_v + 2\mu_v\right)}{\rho_f \left(n\rho_f - \rho\right)},$$

$$a_6 = -\frac{Mn\left(\lambda_e + 2\mu_e\right)}{\rho_f \left(n\rho_f - \rho\right)}. \tag{13}$$

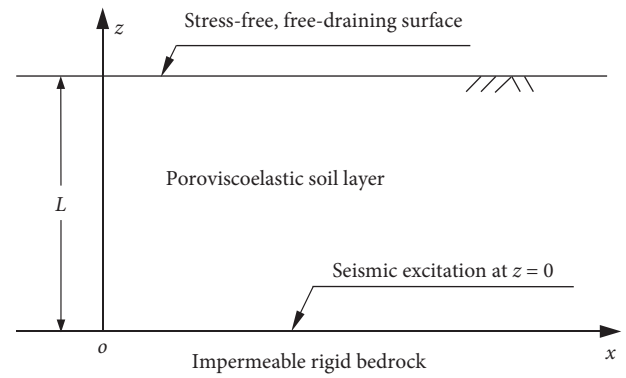

Figure 1: A viscoelastic soil layer subjected to vertical/horizontal earthquake excitation at rigid base.

The seismic response for the steady-state excitation is assumed to take the complex form as

$$u(z,t) = u_0 \exp[i(\omega t - zk)], \tag{14}$$

where u_0 denotes the displacement amplitude, "$\exp[i(\omega t - zk)]$" indicates the spatial and temporal variations of response, where i is the root of -1, ω is the angular frequency, t is time, and k is a complex number.

With aid of equation (13), equation (12) can be rewritten as

$$k^4 + b_1 k^2 + b_2 = 0, \tag{15}$$

in which

$$b_1 = \frac{a_3\omega^2 - a_4 i\omega + a_1 i\omega^3}{a_5 i\omega + a_6},$$

$$b_2 = \frac{\omega^4 - a_2 i\omega^3}{a_5 i\omega + a_6}. \tag{16}$$

The roots for four-order equation (15) are assumed to be $\pm k_{p1}$ and $\pm k_{p2}$, and satisfy $|\mathrm{Re}(k_{p1})| < |\mathrm{Re}(k_{p2})|$, where Re() denotes the real part. Here k_{p1} and k_{p2} are the wave numbers for the two compressional waves, namely, P1 wave and P2 wave in the poroviscoelastic soils.

Without losing generality, the general solution for u in equation (12) is assumed to take the form

$$u(z,t) = \left[c_1 \exp\left(-ik_{p1}z\right) + c_2 \exp\left(ik_{p1}z\right) + c_3 \exp\left(-ik_{p2}z\right) + c_4 \exp\left(ik_{p2}z\right)\right] \exp(i\omega t). \tag{17}$$

The average relative fluid displacement $\overline{w}$ takes a similar form as

$$\overline{w}(z,t) = \left[c_1\eta_1 \exp\left(-ik_{p1}z\right) + c_2\eta_2 \exp\left(ik_{p1}z\right) + c_3\eta_3 \exp\left(-ik_{p2}z\right) + c_4\eta_4 \exp\left(ik_{p2}z\right)\right] \exp(i\omega t), \tag{18}$$

where

$$\eta_1 = \eta_2 = \frac{k_{p1}^2(\lambda + 2\mu + \alpha^2 M) + i\omega k_{p1}^2(\lambda_v + 2\mu_v) - \omega^2\rho}{\omega^2\rho_f - \alpha M k_{p1}^2},$$

$$\eta_3 = \eta_4 = \frac{k_{p2}^2(\lambda + 2\mu + \alpha^2 M) + i\omega k_{p2}^2(\lambda_v + 2\mu_v) - \omega^2\rho}{\omega^2\rho_f - \alpha M k_{p2}^2}. \tag{19}$$

The boundary conditions, as shown in Figure 1, are expressed as

$$z = 0\text{: } u = u_0 \exp(i\omega t), \quad \overline{w} = 0, \tag{20}$$

$$z = L\text{: } p = 0, \quad \sigma'_{zz} = 0. \tag{21}$$

3.2. Horizontal Motion. In this case, the seismically induced pore pressure is assumed to be zero, since no compression is generated when the plastic deformation is ignored. Following similar procedures as equation (12), we obtain

$$\frac{\partial^3 u}{\partial t^3} + a_7\frac{\partial^4 u}{\partial z^2\partial t^2} + a_8\frac{\partial^2 u}{\partial t^2} + a_9\frac{\partial^3 u}{\partial z^2\partial t} + a_{10}\frac{\partial^2 u}{\partial z^2} = 0, \tag{22}$$

in which

$$a_7 = \frac{\mu_v}{n\rho_f - \rho},$$

$$a_8 = -\frac{\rho n b}{(n\rho_f - \rho)\rho_f},$$

$$a_9 = \frac{\mu_v n b + \mu_e \rho_f}{(n\rho_f - \rho)\rho_f}, \tag{23}$$

$$a_{10} = \frac{\mu_e n b}{(n\rho_f - \rho)\rho_f}.$$

Similarly, equation (22) can be further reduced to

$$(i\omega a_9 + a_{10} - \omega^2 a_7)k^2 + \omega^2 a_8 + i\omega^3 = 0. \tag{24}$$

The roots for equation (24) are $\pm k_s$, which indicate the complex wave number for the shear wave (namely, S wave) in the soils. The displacement of solid skeleton takes the form

$$u(z,t) = [c_5 \exp(-ik_s z) + c_6 \exp(ik_s z)]\exp(i\omega t). \tag{25}$$

This case has the boundary conditions expressed as

$$z = 0\text{: } u = u_0 \exp(i\omega t), \tag{26}$$

$$z = L\text{: } \sigma_{xz} = 0. \tag{27}$$

In this way, the coefficients c_j ($j = 1$–6) can be derived by enforcing the boundary conditions. The induced pore stresses and effective stress can be further obtained. In this paper, the amplification factor of the soil layer is defined as the ratio of the response displacement at any depth of the soil layer to that at its rigid base:

$$T(z,t) = \frac{u(z,t)}{u_0}. \tag{28}$$

By choosing $z = L$, the transfer/amplification function for the deposit is given as

$$T(L,t) = \frac{u(L,t)}{u_0}. \tag{29}$$

4. Numerical Results and Discussion

So far, a general theoretical formulation for the dynamic analysis of vertical and horizontal amplification in the soils is briefly presented. In this section, we carry out detailed investigations on the influence of soil properties in various situations. The physical parameters of the viscoelastic soils, which are chosen for numerical calculation, are given in Table 1. Here ξ_v is used as a damping coefficient that denotes the viscosity normalized with respect to the Lamé elastic moduli as $\xi_v = (\lambda_v/\lambda_e) = (\mu_v/\mu_e)$ and assumed to be constant without loss of generality [30, 35]. Besides, the spring constant and dashpot constant also satisfy the following equation [36]:

$$\frac{\Delta W}{W} = 2\pi\frac{\omega\mu_v}{\mu_e}, \tag{30}$$

where ΔW is the area of the hysteresis loop, W is the strain energy stored in a perfectly elastic material, ω is angular frequency, $(\Delta W/W)$ could be obtained experimentally without the need for making any assumption about the mechanism of energy dissipation, and the laboratory tests on soils indicate that $(\Delta W/W)$ is basically irrelevant to vibration frequency [36]. The value of damping coefficient ξ_v can be obtained based on the value of $(\Delta W/W)$ in equation (30). The value of $(\Delta W/W)$ is generally less than 0.8π under the action of machine foundation vibration or earthquake motion [36]. In this study, it is presumed that the maximum of damping coefficient ξ_v is estimated to be 0.1.

4.1. Propagation of Compressional and Shear Waves. The effect of soil viscosity on the wave speeds of P1, P2, and S waves in the frequency range below 30 Hz is depicted in Figure 2. The saturation degree is 100% and the damping coefficient ξ_v is taken to be 0, 0.001, and 0.01, respectively. The wave speeds of P1, P2, and S waves increase with the increase of viscosity, while the influence of soil viscosity on P1 wave is insignificant. When the viscosity of solid skeleton is ignored, that is, $\xi_v = 0$, the model could be reduced to saturated poroelastic medium that obeys classical Biot theory. In this degraded situation, the wave velocities of P1 and S waves are shown to be independent of frequency in the low-frequency range considered in the present paper.

Table 1: Soil properties used in theoretical analysis.

Parameter, notation (unit)	Value
Porosity, n	0.47
Density of solid grain, ρ_s (kg/m^3)	2650
Density of water, ρ_f (kg/m^3)	1000
Permeability, K_p (m/s)	10^{-6}
Absolute fluid pressure, p_{w0} (kPa)	100
Bulk modulus of solid skeleton, K_b (Pa)	4.36×10^7
Bulk modulus of solid skeleton, K_s (Pa)	3.6×10^{10}
Bulk modulus of water, K_w (GPa)	2.0×10^9
Shear modulus of solid skeleton, μ (Pa)	2.61×10^7

However, when the damping coefficient is greater than 0.01, the wave speeds of P1 and S waves increase with the increasing of frequency even for the low frequency. Figure 3 demonstrates the influence of viscosity on the attenuation coefficients which are defined as the imaginary parts of the complex wave numbers. As expected, the waves attenuate faster in the soil with higher viscosity. It is shown that the attenuation coefficients of P1 and S waves, which consider the effect of viscosity ($\xi_v \geq 0.001$), are several orders of magnitude larger than those in elastic medium ($\xi_v = 0$). This may be due to the fact that the propagations of P1 wave and S wave are closely related to the viscoelastic behaviour of solid skeleton.

The existing experimental results have revealed that partial saturation may significantly reduce the velocity of the P-wave [37, 38]. In certain situation, the soil below groundwater level may not be completely saturated even if the saturation degree is very high. Figure 4 depicts the influence of viscosity on the propagation velocities of seismic waves in the near-surface soils with various saturation degrees. The saturation degree S_r is taken to be 95%, 99%, 99.9%, and 100%, respectively. It is shown that even a slight amount of air could significantly reduce the bulk modulus of fluid in terms of stiffness and absolute pore pressure, as given in equation (5). Hence the P-wave velocity decreases drastically with even a small decrease below full saturation [8]. For example, in the case of $\xi_v = 0.001$, the velocity of P1 wave reaches the maximum at fully saturated state, about 1480 m/s, while it drops to about 230 m/s in the case of $S_r = 95\%$. For S waves, as expected, the effect of saturation degree is negligible. As shown in Figure 4(a), the viscosity has little effect on the wave speed of P1 wave in fully saturated soils. On the contrary, the viscosity has significant effect on the speed of P2 wave in the case of complete saturation. In addition, the wave speed of S wave increases markedly when the damping coefficient is greater than 0.01.

Figure 5 illustrates the effect of viscosity on the attenuation coefficients of three different seismic waves in the cases with various saturation degrees. P1 wave attenuates faster in the soils with greater viscosity in the completely saturated case. However, it attains the maximum and then decreases with damping coefficient when the soil is partly saturated. The attenuation coefficient of S wave firstly increases with damping coefficient, reaches the peak value near $\xi_v = 0.03$, and then decreases, while that of P2 wave is almost independent of damping coefficient at different saturation degrees.

4.2. Amplification of Soil Displacement. In this section, the effects of soil viscosity on the seismic vertical/horizontal amplification in a soil layer are further investigated. The seismic excitation at the surface of rigid bedrock is assumed to be vertical and horizontal, respectively. The distributions of amplification factor with depth for three specified saturation degrees ($S_r = 99\%$, 99.9%, and 100%) in the case of vertical motion are given in Figure 6. The thickness of soil layer is 20 m and the frequency is 3 Hz. In the case of full saturation, the distribution of amplification factor with depth is demonstrated to be independent of soil viscosity. However, the soil viscosity in nearly saturated soils is shown to reduce the amplification factor at any depth of the soil especially when the damping coefficient is greater than 0.01. Figure 7 illustrates the distribution of amplification factor with depth in the case of horizontal earthquake action. Since the horizontal motion of soil is associated with the vertical propagation of shear waves, the effect of saturation degree is negligible. As the damping coefficient increases, the fluctuation of horizontal amplification factor with respect to soil depth becomes more obscure.

Figure 8 illustrates the variation of the vertical amplification factor at soil surface with frequency in the cases of three different saturation degrees. The frequency is assumed to be 5 Hz. A noticeable difference is found between the cases of incomplete saturation and the case of full saturation. When the saturation degree is only slightly below full saturation, the peak frequency is substantially shifted to the low-frequency end. This performance is reasonable, since the air inclusion can lead to a significant decrease in P-wave velocity, which has been discussed in the preceding section. Therefore, since the ground soil in engineering practice is always partly saturated, the fundamental frequency (the lowest peak frequency) of vertical amplification factor at surface will appear in the relative low-frequency range. The peak value of amplification factor at surface is also shown to decrease significantly with the increasing of soil viscosity, though the soil viscosity will not affect the peak frequency. In the unsaturated soils with high viscosity, such as $S_r = 99\%$ and $\xi_v = 0.01$, the vertical amplification factor at the soil surface decreases sharply as the frequency becomes greater than the second peak frequency. As depicted in Figure 9, the horizontal amplification factor at soil surface is dependent on saturation degree and the fundamental frequency is lower than that for vertical amplification. Now it can be concluded that a poroelastic model ($\xi_v = 0$) could always overestimate the motion amplifications in both vertical and horizontal directions.

For the earthquake loading, the frequencies of interest are usually not high. For example, the predominant

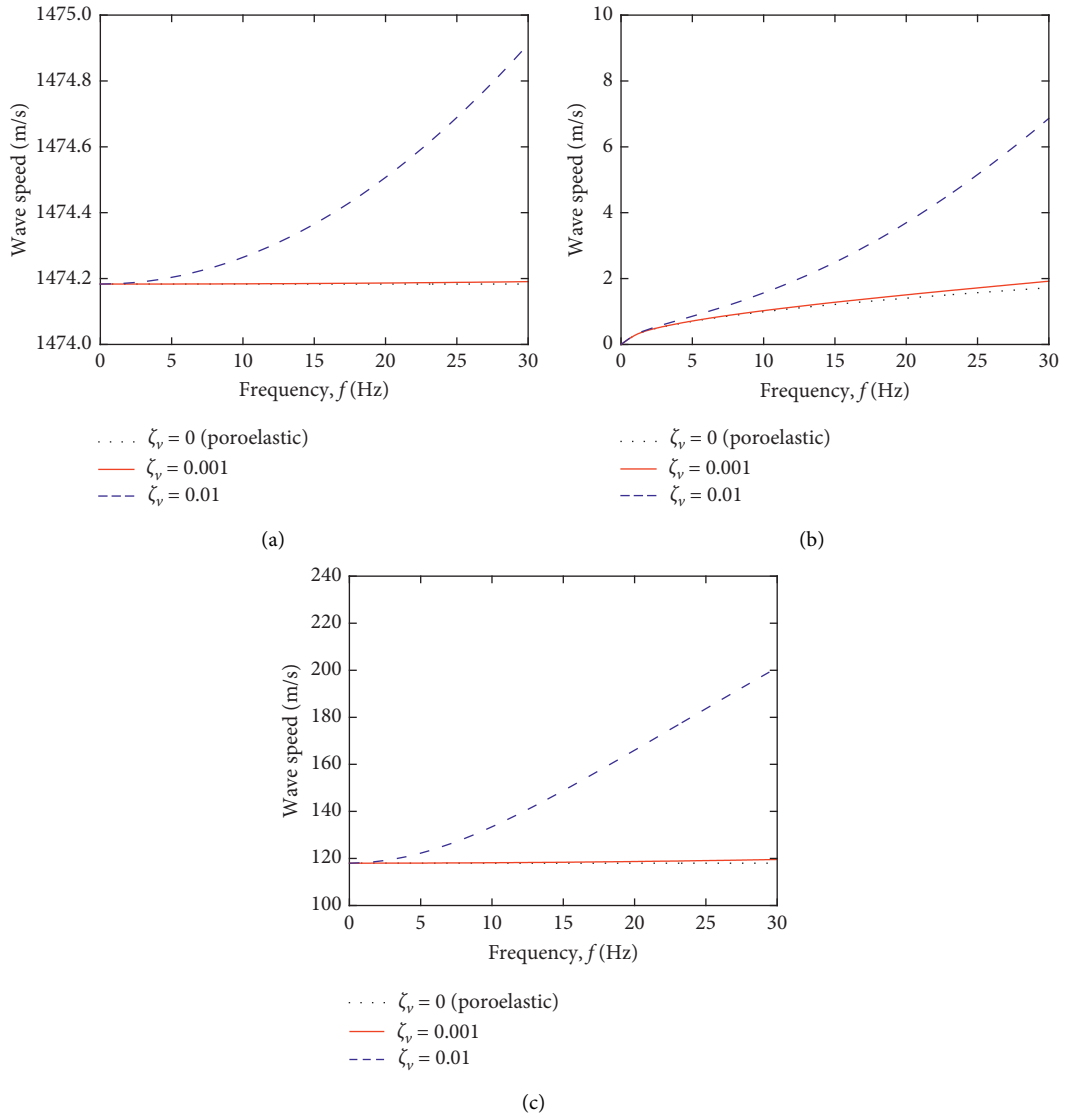

Figure 2: Variation of wave speeds of P1, P2, and S waves with frequency. (a) P1 wave. (b) P2 wave. (c) S wave.

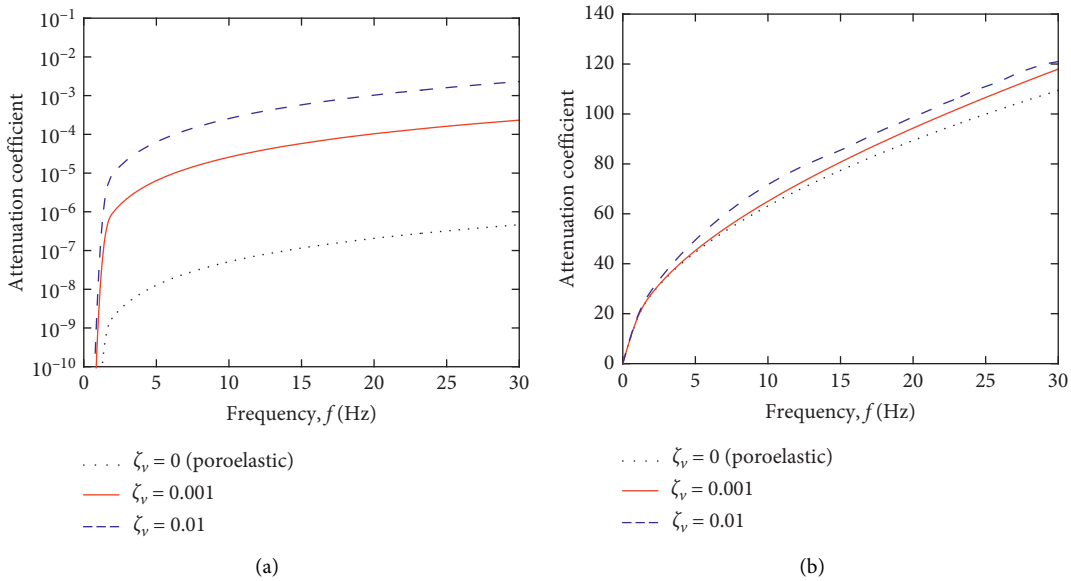

Figure 3: Continued.

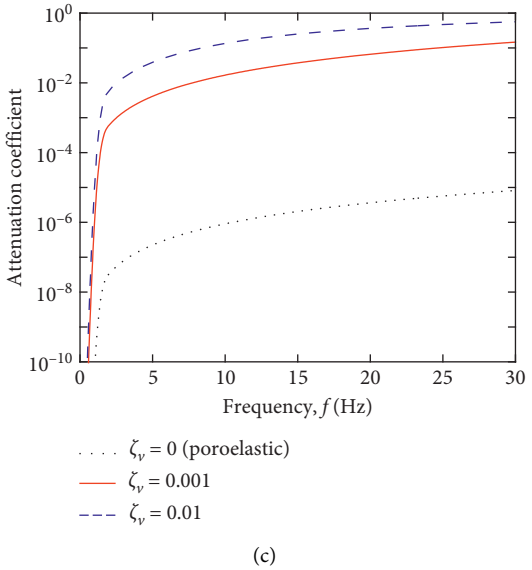

(c)

Figure 3: Variation of attenuation coefficients of P1, P2, and S waves with frequency. (a) P1 wave. (b) P2 wave. (c) S wave.

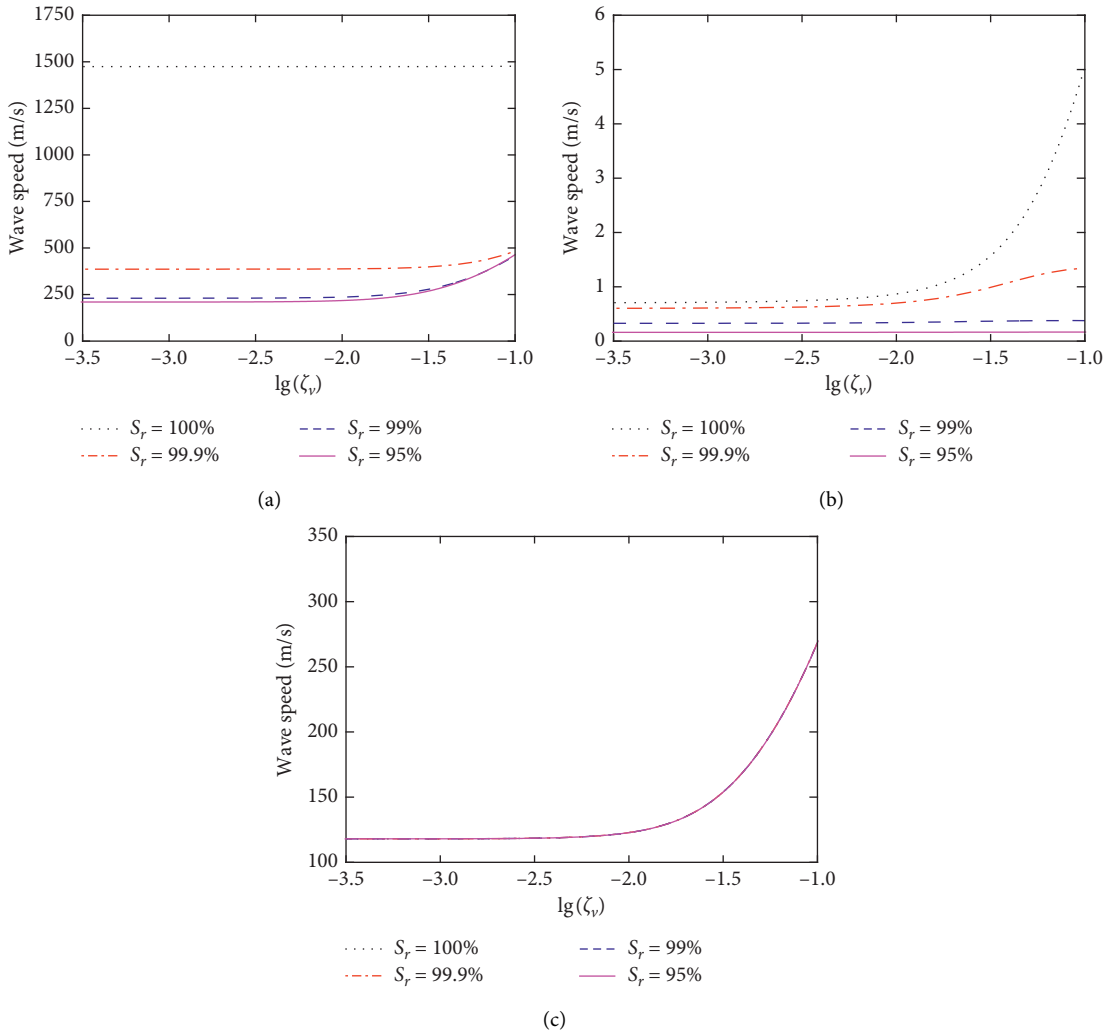

(a) (b)

(c)

Figure 4: Variation of wave speeds of P1, P2, and S waves with damping coefficient ξ_v. (a) P1 wave. (b) P2 wave. (c) S wave.

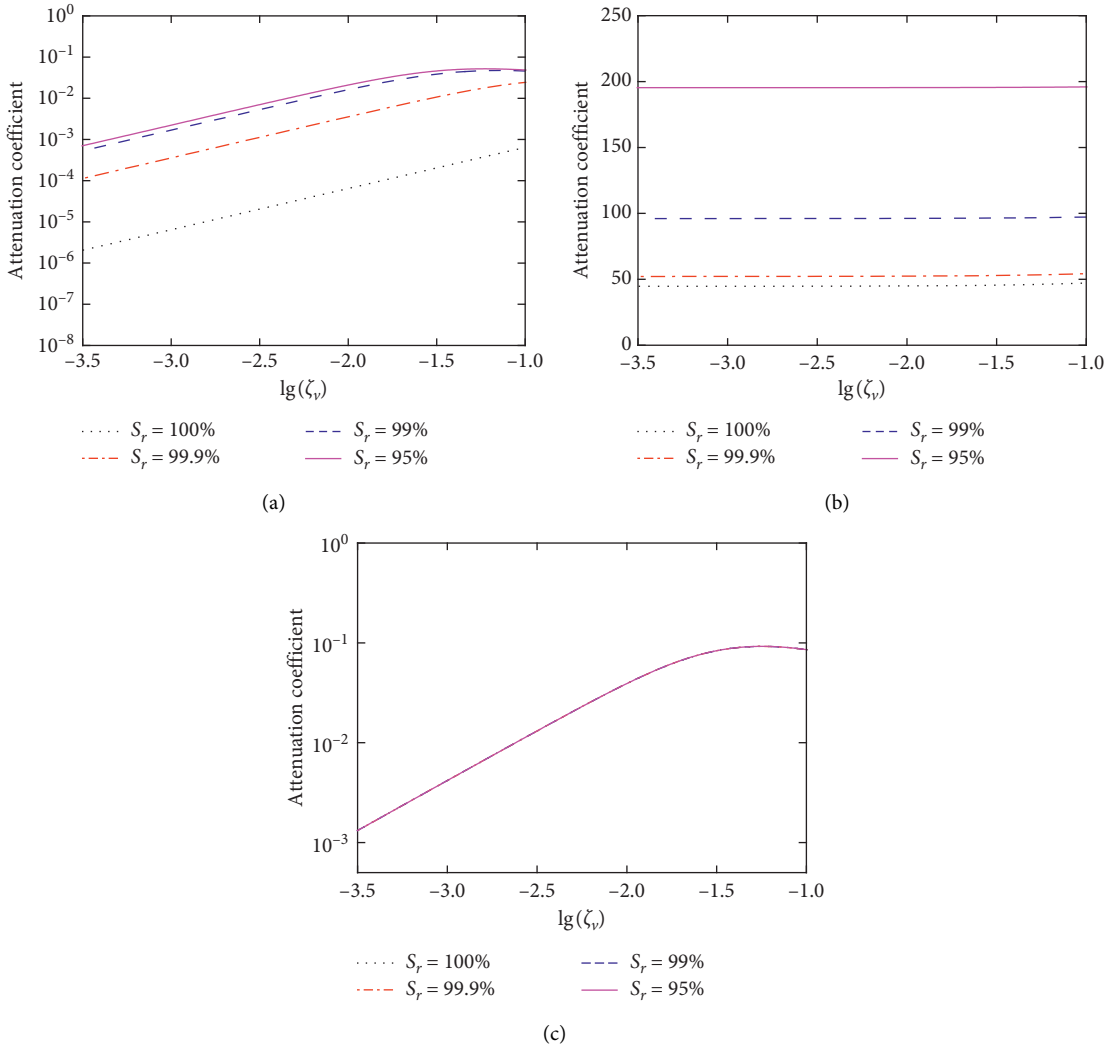

Figure 5: Variation of attenuation coefficients of P1, P2, and S waves with damping coefficient ξ_v. (a) P1 wave. (b) P2 wave. (c) S wave.

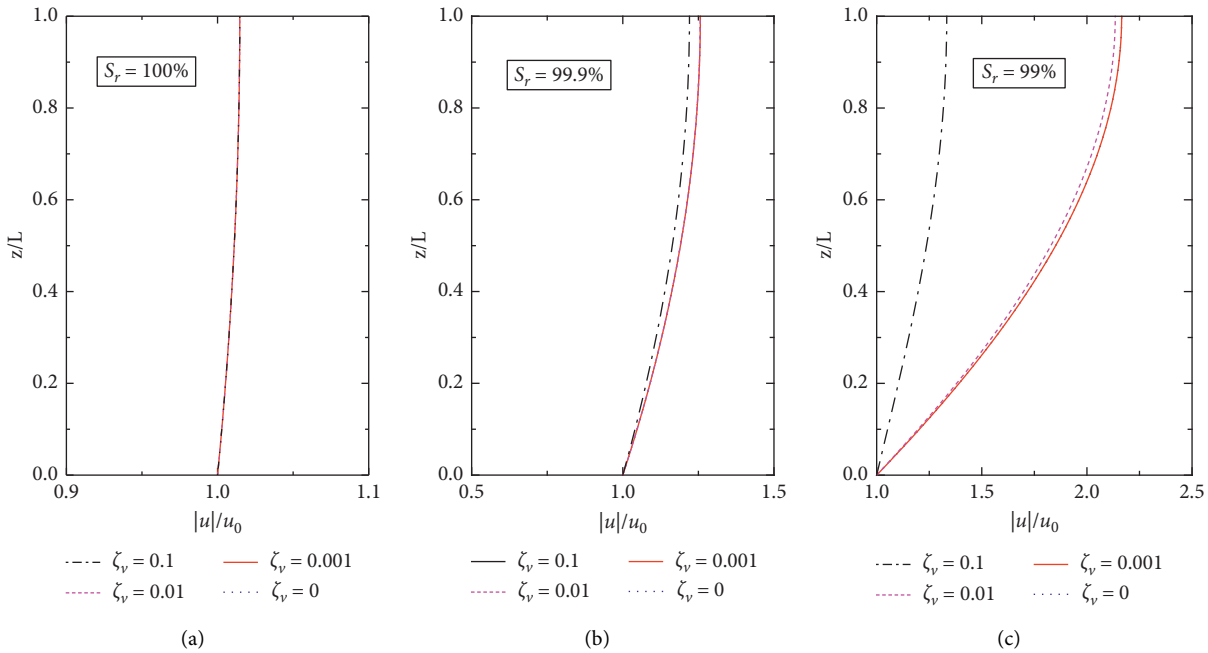

Figure 6: Distributions of amplification factor with depth for three specified saturation degrees (vertical motion).

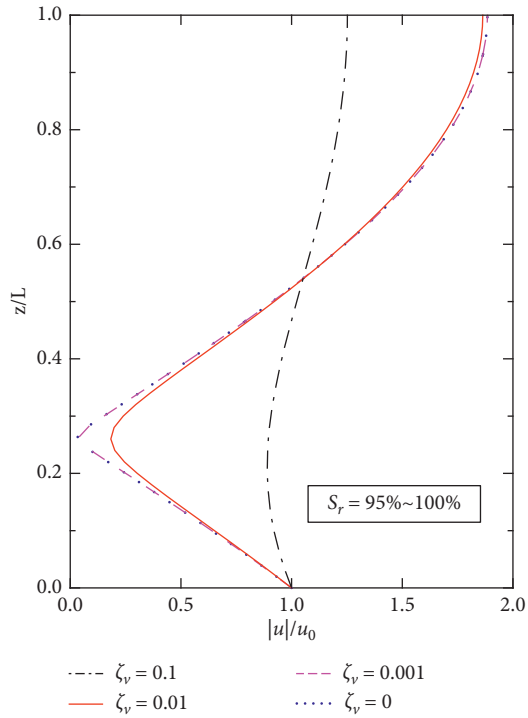

Figure 7: Distribution of amplification factor with depth (horizontal motion).

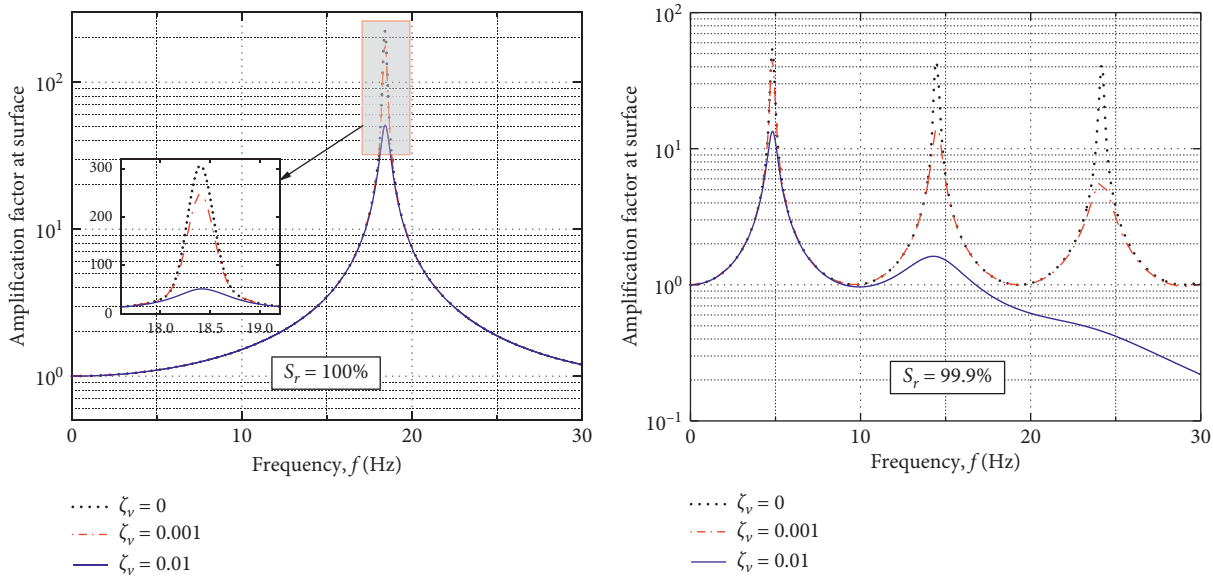

Figure 8: Continued.

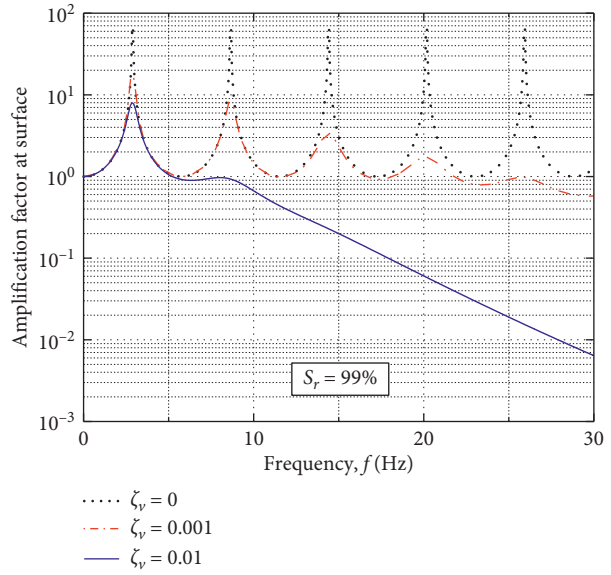

(c)

Figure 8: Variation of amplification factor at surface with frequency at three cases of different saturation degrees (vertical motion).

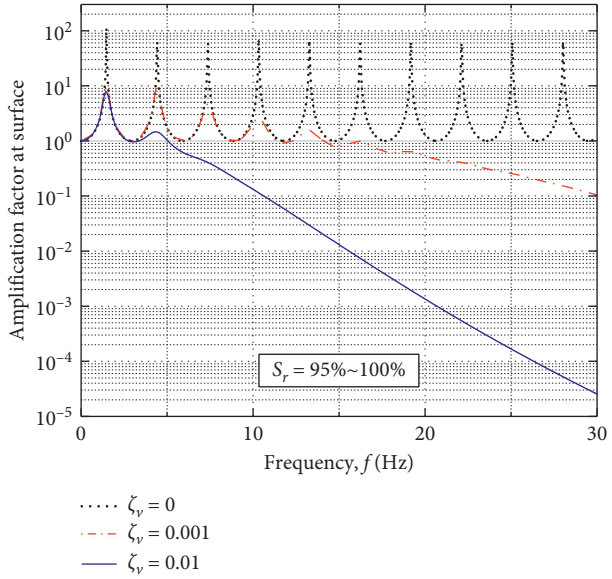

Figure 9: Variation of amplification factor at surface with frequency (horizontal motion).

frequency in vertical earthquake recorded at the array site is around 5 Hz [21]. Therefore, a better view of the amplification factor at surface in a low-frequency range ($f \leq 10$ Hz) is given in Figure 10 for $S_r = 100\%$. For the vertical amplification, the influence of damping coefficient on the variation of amplification factor at surface is more remarkable at higher frequency. In addition, the effect of damping coefficient is negligible when $\xi_v \leq 0.1$ in this fully saturated case. Moreover, the horizontal and vertical amplifications at surface approach 1.0 when the damping coefficient is high enough.

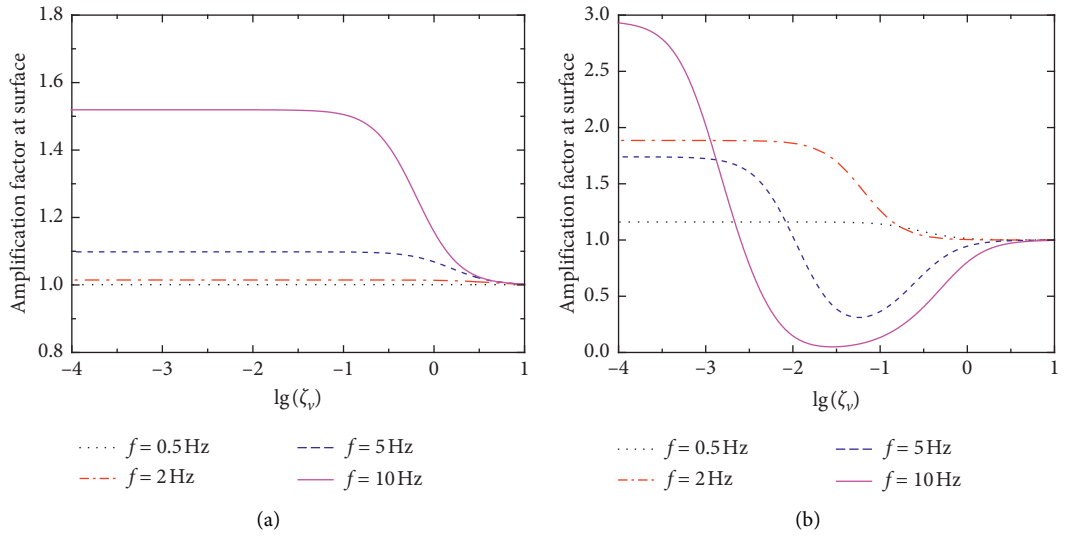

Figure 10: Variation of amplification factor at surface with damping coefficient ξ_v. (a) Vertical motion. (b) Horizontal motion.

5. Conclusions

In this paper, an analytical study is presented to identify viscosity effect of soil skeleton on dynamic behaviour of the soil layer under the action of vertical/horizontal earthquake excitation at the underlying rigid base. The Kelvin–Voigt stress-strain relationship is incorporated into the governing equations. The seismic-induced displacements depending on the soil properties, thickness of soil layer, and seismic frequency are derived. The main conclusions are summarized as follows:

(1) The soil viscosity has noticeable impact on the wave speed of P2 wave, while the influence is insignificant on the P1 wave. The wave speed of S wave increases with damping coefficient, which is independent of saturation degree.

(2) The seismic waves attenuate faster in the soil with higher viscosity. The attenuation coefficients of P1 and S waves, which consider the effect of soil viscosity, are several orders of magnitude greater than that in elastic medium.

(3) The distribution of vertical amplification factor with depth is demonstrated to depend on the soil viscosity considered in this paper only in the unsaturated soil layer. The fluctuation of horizontal amplification factor with respect to soil depth becomes more obscure as the damping coefficient increases.

(4) The peak frequency for the vertical amplification factor at soil surface is substantially shifted to the low frequency end even if the saturation degree is only slightly below 100%. The peak value of amplification factor decreases markedly with the increasing of soil viscosity, though the soil viscosity will not affect the peak frequency.

(5) The influence of damping coefficient on the variation of vertical amplification factor at soil surface is more remarkable at higher frequency. Both the horizontal and vertical amplifications at surface approach 1.0 when the damping coefficient is high enough.

Data Availability

No data were used to support this study.

Conflicts of Interest

The authors declare that there are no conflicts of interest regarding the publication of the article.

Acknowledgments

This research was supported by the National Natural Science Foundation of China (Grants nos. 41877243 and 41502285), Natural Science Foundation of Jiangsu Province (Grant no. BK20150952), Nanning Science Research And Technology Development Plan (Grant no. 20173160-6), and the China Postdoctoral Science Foundation (Grant no. 2017M623294XB).

References

[1] P. Meunier, N. Hovius, and J. A. Haines, "Topographic site effects and the location of earthquake induced landslides," *Earth and Planetary Science Letters*, vol. 275, no. 3-4, pp. 221–232, 2008.

[2] V. Di Fiore, "Seismic site amplification induced by topographic irregularity: results of a numerical analysis on 2D synthetic models," *Engineering Geology*, vol. 114, no. 3-4, pp. 109–115, 2010.

[3] M. Sugito, F. Oka, A. Yashima, Y. Furumoto, and K. Yamada, "Time-dependent ground motion amplification characteristics at reclaimed land after the 1995 Hyogoken Nambu earthquake," *Engineering Geology*, vol. 56, no. 1-2, pp. 137–150, 2000.

[4] L. G. Baise, J. Kaklamanos, B. M. Berry, and E. M. Thompson, *Soil Amplification with a Strong Impedance Contrast*, vol. 202Boston, MA, USA, 2016.

[5] N. Ma, G. Wang, T. Kamai, I. Doi, and M. Chigira, "Amplification of seismic response of a large deep-seated landslide in Tokushima, Japan," *Engineering Geology*, vol. 249, pp. 218–234, 2019.

[6] N. Liu, X. Feng, Q. Huang et al., "Dynamic characteristics of a ground fissure site," *Engineering Geology*, vol. 248, pp. 220–229, 2019.

[7] M. Kham, J.-F. Semblat, and N. Bouden-Romdhane, "Amplification of seismic ground motion in the Tunis basin: numerical BEM simulations vs experimental evidences," *Engineering Geology*, vol. 155, pp. 80–86, 2013.

[8] H.-Y. Zhao, J.-F. Zhu, J.-H. Zheng, and J.-S. Zhang, "Numerical modelling of the fluid-seabed-structure interactions considering the impact of principal stress axes rotations," *Soil Dynamics and Earthquake Engineering*, vol. 136, Article ID 106242, 2020.

[9] W. Chen, Y. Huang, Z. Wang, R. He, G. Chen, and X. Li, "Horizontal and vertical motion at surface of a gassy ocean sediment layer induced by obliquely incident SV waves," *Engineering Geology*, vol. 227, pp. 43–53, 2017.

[10] W. Chen, D. Jeng, G. Chen, H. Zhao, R. He, and H. Gao, "Momentary liquefaction of porous seabed under vertical seismic action," *Applied Ocean Research*, vol. 73, pp. 80–87, 2018.

[11] W.-Y. Chen, Z.-H. Wang, G.-X. Chen, D.-S. Jeng, M. Wu, and H.-Y. Zhao, "Effect of vertical seismic motion on the dynamic response and instantaneous liquefaction in a two-layer porous seabed," *Computers and Geotechnics*, vol. 99, pp. 165–176, 2018.

[12] G. Fan, L. M. Zhang, X. Y. Li, R. L. Fan, and J. J. Zhang, "Dynamic response of rock slopes to oblique incident SV waves," *Engineering Geology*, vol. 247, pp. 94–103, 2018.

[13] W. Chen, D. Jeng, W. Chen, G. Chen, and H. Zhao, "Seismic-induced dynamic responses in a poro-elastic seabed: solutions of different formulations," *Soil Dynamics and Earthquake Engineering*, vol. 131, Article ID 106021, 2020.

[14] S. Yang, B. Leshchinsky, K. Cui, F. Zhang, and Y. Gao, "Influence of failure mechanism on seismic bearing capacity factors for shallow foundations near slopes," *Geotechnique*, 2020.

[15] J. Yang and X. R. Yan, "Factors affecting site response to multi-directional earthquake loading," *Engineering Geology*, vol. 107, no. 3-4, pp. 77–87, 2009.

[16] A. J. Papazoglou and A. S. Elnashai, "Analytical and field evidence of the damaging effect of vertical earthquake ground motion," *Earthquake Engineering and Structural Dynamics*, vol. 25, no. 2, pp. 1109–1137, 1996.

[17] A. Elgamal and L. He, "Vertical earthquake ground motion records: an overview," *Journal of Earthquake Engineering*, vol. 8, no. 5, pp. 663–697, 2004.

[18] Q. S. Chen, G. Y. Gao, and J. Yang, "Dynamic response of deep soft soil deposits under multidirectional earthquake loading," *Engineering Geology*, vol. 121, no. 1-2, pp. 55–65, 2011.

[19] R. W. Day, *Geotechnical Earthquake Engineering Handbook*, McGraw-Hill Professional, New York, NY, USA, 1996.

[20] J. Ingles, J. Darrozes, and J. Soula, "Effects of the vertical component of ground shaking on earthquake-induced landslide displacements using generalized Newmark analysis," *Engineering Geology*, vol. 86, no. 2-3, pp. 134–147, 2006.

[21] J. Yang, T. Sato, and X.-S. Li, "Nonlinear site effects on strong ground motion at a reclaimed island," *Canadian Geotechnical Journal*, vol. 37, no. 1, pp. 26–39, 2000.

[22] M. A. Biot, "Theory of propagation of elastic waves in a fluid-saturated porous solid," *The Journal of the Acoustical Society of America*, vol. 28, no. 4, pp. 168–191, 1956.

[23] O. C. Zienkiewicz, C. T. Chang, and P. Bettess, "Drained, undrained, consolidating and dynamic behaviour assumptions in soils," *Géotechnique*, vol. 30, no. 4, pp. 385–395, 1980.

[24] S. Okusa, "Wave-induced stresses in unsaturated submarine sediments," *Géotechnique*, vol. 35, no. 4, pp. 517–532, 1985.

[25] K. Zhao, H. Xiong, G. Chen, H. Zhuang, and X. Du, "Cyclic characterization of wave-induced oscillatory and residual response of liquefiable seabed," *Engineering Geology*, vol. 227, pp. 32–42, 2017.

[26] W. Chen, D. Fang, G. Chen, D. Jeng, J. Zhu, and H. Zhao, "A simplified quasi-static analysis of wave-induced residual liquefaction of seabed around an immersed tunnel," *Ocean Engineering*, vol. 148, pp. 574–587, 2018.

[27] J. R. Hall and F. E. Richart, "Dissipation of elastic wave energy in granular soils," *Journal of the Soil Mechanics and Foundations Division: SM*, vol. 89, no. 6, pp. 27–56, 1963.

[28] E. A. Ellis, K. Soga, M. F. Bransby, and M. Sato, "Resonant column testing of sands with different viscosity pore fluids," *Journal of Geotechnical and Geoenvironmental Engineering*, vol. 126, no. 1, pp. 10–17, 2000.

[29] J. P. Bardet, "A viscoelastic model for the dynamic behavior of saturated poroelastic soils," *Journal of Applied Mechanics*, vol. 59, no. 1, pp. 128–135, 1992.

[30] K.-h. Xie, G.-b. Liu, and Z.-y. Shi, "Dynamic response of partially sealed circular tunnel in viscoelastic saturated soil," *Soil Dynamics and Earthquake Engineering*, vol. 24, no. 12, pp. 1003–1011, 2004.

[31] W. Wu, J. B. Zhu, and J. Zhao, "Dynamic response of a rock fracture filled with viscoelastic materials," *Engineering Geology*, vol. 160, pp. 1–7, 2013.

[32] A. C. Eringen, *Mechanics of Comtinua*, R. Krveqer, Ed., Huntington Press, New York, NY, USA, 1980.

[33] A. Verruijt, "Elastic storage of aquifers," in *Flow through Porous Media*, R. J. M. De Wiest, Ed., pp. 331–376, Academic Press, New York, NY, USA, 1969.

[34] A. Gajo, "Influence of viscous coupling in propagation of elastic waves in saturated soil," *Journal of Geotechnical Engineering*, vol. 121, no. 9, pp. 636–644, 1995.

[35] G. Militano and R. K. N. D. Rajapakse, "Dynamic response of a pile in a multi-layered soil to transient torsional and axial loading," *Géotechnique*, vol. 49, no. 1, pp. 91–109, 1999.

[36] A. S. Veletsos and B. Verbič, "Vibration of viscoelastic foundations," *Earthquake Engineering and Structural Dynamics*, vol. 2, no. 2, pp. 87–102, 1973.

[37] G. C. Sills, S. J. Wheeler, S. D. Thomas, and T. N. Gardner, "Behaviour of offshore soils containing gas bubbles," *Géotechnique*, vol. 41, no. 2, pp. 227–241, 1991.

[38] N. F. Allen, R. D. Woods, and F. E. Richart, "Fluid wave propagation in saturated and nearly saturated sands," *Journal of Geotechnical and Geoenvironmental Engineering*, vol. 106, no. 5, pp. 701-702, 1981.